Online Appendix

A Model for emissions

I require a model that maps changes in the number and type (i.e. the complexity) of the wells in each location into changes in global carbon dioxide emissions. I do this in three steps:

1. Map matches into oil and gas production in the deepwater market.

2. Map changes in oil and gas production in the deepwater market into changes in global production and consumption globally, which involves accounting for equilibrium effects.

3. Map changes in global oil and gas consumption into changes in global carbon dioxide emissions.

Note that, as I set out in more detail below, step 2 and step 3 reduce down to multiplying changes in oil and gas production in the deepwater market by a scale factor which is calibrated based on the best-available empirical estimates. I evaluate the counterfactuals in the paper mainly by either the *percent changes* in emissions, or leakage statistics that are the change in emissions generated in the unregulated markets divided by the change in emissions generated in the regulated market. These metrics are scale-free measures, and so do not rely on specific assumptions for the scale factors applied in steps 2 and 3.

1. Map matches into oil and gas production in the deepwater market
For the first model, I run the regression:

$$\text{oil production}_i = \beta_0 + \beta_1 \text{well complexity}_i + \epsilon_i \tag{A-1}$$

which exploits the strong relationship between complex wells and increased oil production. In order to measure oil production, I take the average number of barrels produced per day

Figure A-1: Relationship between oil production and well complexity
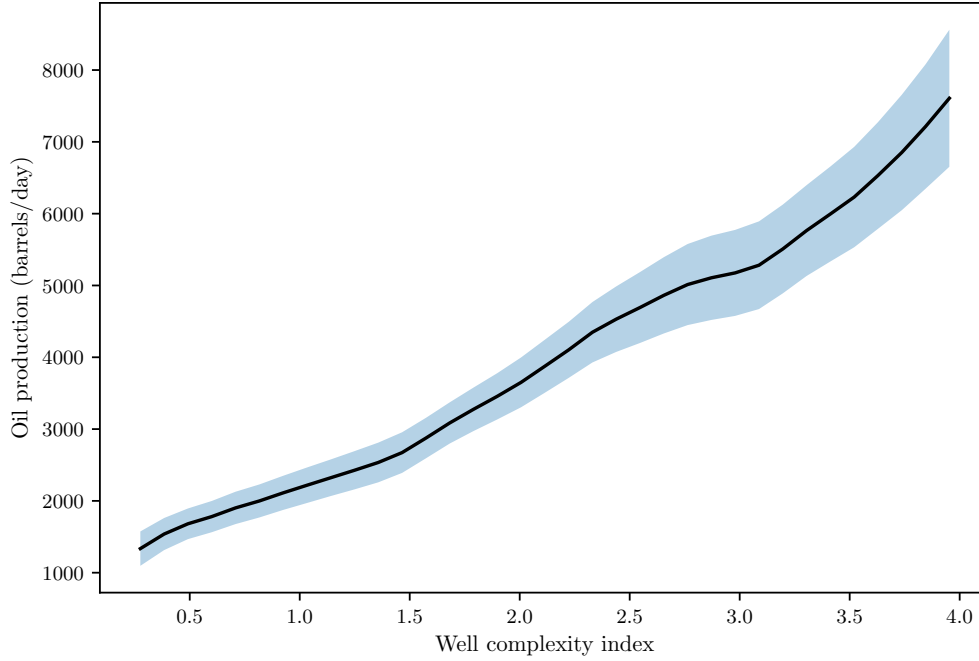
Note: Shaded area is the 95% confidence interval.

for the first 10 years of production. The results from this regression are $\beta_0 = 358.1(751.5)$ and $\beta_1 = 1666.0(276.6)$ (standard errors in brackets) and the sample size is for 143 wells where there is both production and well complexity data. I plot a local polynomial regression of this relationship in Figure A-1.

2. Map changes in oil and gas production in the deepwater market into changes in global production and consumption globally

In this step I follow Ahlvik et al. (2022). Assume that the supply and demand curves in the world market are well-approximated (locally) by constant elasticity of supply and demand curves. Then, a partial equilibrium change of an extra barrel produced in the deepwater market will result in a total equilibrium change to the equilibrium barrels produced and consumed worldwide of $-e_D/(-e_D + e_S)$. Here, e_D and e_S denote global demand and supply elasticities. Consistent with Ahlvik et al. (2022) I use a value of $e_S = 1.96$ as the long-term supply elasticity. Furthermore, as detailed in Ahlvik et al. (2022), demand elasticities from $e_D = -0.2$ to $e_D = -0.5$ are used in the literature. As

previously discussed, since the main estimates that I report in the counterfactuals are scale-free measures (such as percentage changes in emissions), these results are robust to assumptions on e_D and e_S. Therefore, for simplicity, I compute the total change using the midpoint demand elasticity of $e_D = -0.35$.

3. Map changes in global oil and gas consumption into changes in global carbon dioxide emissions.

In this step I convert this global change in output to carbon emissions by scaling by the EPA's Greenhouse Gases Equivalencies Calculator. This factor is 0.43 metric tons carbon dioxide/barrel oil.[1]

B   Data construction

I use several datasets for the analysis:

- Rigzone data of rig status updates and contracts

- Permit, borehole, and production data, from the BSEE (Bureau of Safety and Environmental Enforcement)

- CERDI dataset of bilateral distances between locations

I explain first how I clean the raw Rigzone data. I then explain how I perform a merge between the BSEE data and the Rigzone data to get the data on contracts and details of the projects under each contract in the US market. Finally, I explain how I construct key metrics from the cleaned data like rig utilization.

B.1   Cleaning the Rigzone data

As mentioned in the data section (Section 2.1), offshore drilling can be split into two broad categories. The first category is shallow-water drilling which is undertaken in water depths of less than 500ft using 'jackup' rigs which extend their legs to the seabed.

---

[1]The calculator is here: https://www.epa.gov/energy/greenhouse-gases-equivalencies-calculator-calculations-and-references

The second category is deepwater drilling with is undertaken in water depths of more than 500ft using 'floater' rigs (drillships and semi-submersibles) which anchor themselves to the seabed. These two categories of drilling are treated by practitioners as essentially separate markets. This is due to, for example, the differences in rig technology, and the fact that the oil and gas wells drilled by rigs in the deepwater are typically much more complex, costly, and productive, than wells in shallow water. In this paper I cut the data just to the deepwater market for the years 2005-2016 where the number of contracts per year appears to be relatively stable.

Although most rigs operate under relatively short-run contracts, a small number of rigs operate under extremely long-run contracts for a single oil company (e.g. a 10 year contract). I delete rigs that operate under contracts that are longer than 2 years, treating these very long-run contracts as essentially a different type of market than those deepwater rigs which perform short-run work. Specifically, I delete 236 contracts that are longer than 2 years, comprising 11.2% of the total number of contracts (and reducing the total number of contracts from 2109 to 1873).

B.2 Merging the Rigzone data with the BSEE data

Critical to my estimation strategy is data that links rig and well characteristics to contract prices (and other contract details). In the US market I have data on both well characteristics (from the BSEE) and contract details (from Rigzone). In this section I describe how I merge these two datasets.

I begin with a dataset of 375 contracts for the US market, and 781 wells. I successfully match 478 wells with contracts, and collapse these contracts to 183 contracts (many contracts contain multiple wells and for these cases I use the average complexity of the matched wells). Why are some wells and contracts not matched? Sometimes the rig name is recorded differently between the well dataset and the contract dataset, for example the rig's name might change and the current name may be used in the contract dataset, whereas the original name is used in the well dataset. I try to connect as many rig and well names as possible by including previous rig names and accounting for simple

typographical differences between the names in the datasets.

Finally, I delete contracts which may have been affected by the moratorium, resulting in a final dataset of 143 contracts. I use these contracts for the auxiliary regression in the model estimation. Note that for the graphs in Figure (4) I use the 'uncollapsed' sample of 478 wells. Also note that for many metrics such as average prices, utilization etc, I do not require the matched contracts and so where possible I use the full sample of contracts.

B.3 Constructing metrics

In this subsection I describe how I construct metrics that I use in the estimation from the cleaned Rigzone data.

B.3.1 Rig relocations

I construct rig relocations simply by looking at changes in rig statuses (for example, a rig is in one region in one status and then in the next status it is in a different region). Typically, these relocations are that the rig is drilling in one region and then moves to drill in a different region. However, there are some exceptions to this. Notably, I include several movements from a shipyard (e.g. the rig is 'Under Construction' in Asia) to a different region (e.g. the rig is then 'Drilling' in USA) as a relocation. My justification for including this as a relocation choice is that these rigs could have alternatively just remained and drilled in the field in the region in which they were constructed (my definition of a region is large enough that it is always a possibility that this could occur) or potentially could have chosen to move after construction to a different location. Therefore, I assume that these relocations contain useful information about the relative costs and benefits of drilling in different locations and so include them in the relocation data.

B.3.2 Rig utilization

Rig utilization is defined as the average proportion of time that a rig is being used in a given location. I begin by converting the statuses of every rig (which in the raw data look like, for example, a rig is "Drilling" between a block of two dates at a given day-rate for a particular oil and gas company in a particular location) into a daily dataset of activity

at the individual rig level, for every day between 2005-2016. I then classify these daily statuses into whether a rig is utilized or not. I consider a rig utilized if it is in the statuses of "Drilling", "Workover", "Production", "Modification", "Inspection". I consider the total number of rigs in a location (the denominator for utilization) as all these statuses except if a rig is "Under Construction" or "Cold Stacked" (mothballed). The main status of rigs not utilized in a location is that they are "Ready Stacked" (staffed and ready to drill with little delay).

Note that to compute the moments in estimation, I delete the period of time when the US drilling moratorium was active for the entire world market. This is because during this period contracts were cancelled using 'force majeure' provisions after the moratorium; outside of the moratorium I observe no other instances of cancelled contracts in the data.

B.3.3 Well complexity: the mechanical risk index

This section is written exactly as in Vreugdenhil (2023). In that paper this section draws directly from Kaiser (2007). The Mechanical Risk Index was developed by Conoco engineers in the 1980s (Kaiser (2007)). The idea behind the index is to collapse the many dimensions that a well can differ on into a one-dimensional ranking of well complexity. Well complexity is directly related to the cost of drilling a well: these wells run an increased risk of technical issues which may require new materials or result in blowouts.

The Mechanical Risk Index is computed by first computing 'component factors':

$$\phi_1 = \left(\frac{TD+WD}{1000}\right)^2$$
$$\phi_2 = \left(\frac{VD}{1000}\right)^2 \left(\frac{TD+HD}{VD}\right)$$
$$\phi_3 = (MW)^2 \left(\frac{WD+VD}{VD}\right)$$
$$\phi_4 = \phi_1 \sqrt{NS + \frac{MW}{(NS)^2}}$$

Here TD is total depth in feet, WD is water depth in feet, VD is vertical depth in feet,

MW is mud weight in ppg, NS is the number of strings.

Next 'key drilling factors' are computed. These are: $\psi_1 = 3$ if there is a horizontal sections; $\psi_2 = 3$ if there is a J-curve; $\psi_3 = 2$ if there is an S-curve; ψ_4 if there is a subsea well; $\psi_5 = 1$ if there is an H_2S/CO_2 environment; $\psi_6 = 1$ if there is a hydrate environment; $\psi_7 = 1$ if there is a depleted sand section; $\psi_8 = 1$ if there is a salt section; $\psi_9 = 1$ if there is a slimhole, $\psi_{10} = 1$ if there is a mudline suspension system installed; $\psi_{11} = 1$ if there is coring; $\psi_{12} = 1$ if there is shallow water flow potential; $\psi_{13} = 1$ if there is riserless mud to drill shallow water flows; $\psi_{14} = 1$ if there is a loop current.

The Mechanical Risk Index is then computed as:

$$MRI = \left(1 + \frac{\sum_j \psi_j}{10}\right) \sum_i \psi_i$$

In my data I have excellent information for all wells on TD, WD, VD, HD using the BSEE permit data and the BSEE borehole data. I have data for MW, NS for a subset of wells and I impute the remainder based on geological proximity (whether they are in the same 'field') - based on the fact that geological conditions are usually similar for nearby wells.

Computing the 'key drilling factors' ψ_j presents a greater challenge because the data are either not recorded (e.g. if there is shallow water flow potential) or would need to be imputed from well velocity surveys (e.g. if there is an S-curve). Rather than guess I set all $\psi_j = 0$. The implication for the index is that there will be a less accurate measure of complexity which will result in measurement error.

C   Algorithms

C.1   Algorithm for computing the supply-side equilibrium

I compute the parameters $\delta_{l,y}, \sigma_\epsilon, b_{stay}$ using maximum likelihood. I compute the likelihood function for each guess of the parameters as follows. Denote the k-th iteration of the value functions for a searching rig and an unemployed rig, respectively, by $V_{l,y}^k, U_{l,y}^k$. Then, I compute the likelihood using predicted choice probabilities using the following

algorithm:

1. Guess initial value functions at iteration $k = 0$: $V_{l,y}^0, U_{l,y}^0$.

2. Using Equation (5), update the value of searching in each location l, for each type of rig y, $V_{l,y}^{k+1}$. Use the empirical probabilities of matching in each location as the $q_{l,y}^{capital}$.

3. Using Equation (4), update the value of unemployment in each location l, for each type of rig y, $U_{l,y}^{k+1}$.

4. Repeat from Step 2. until the value functions converge.

5. Compute predicted choice probabilities for moving from location l to l' for a rig of type y, using $V_{l,y}$ and Equations (A-2) and (A-3). These choice probabilities are:

$$P_{l,l',y} = \frac{\exp\left(\left(-c_d d_{l,l'} + \beta V_{l',y}\right)/\sigma_\epsilon\right)}{\exp\left(\left(b_{stay} + \beta V_{l,y}\right)/\sigma_\epsilon\right) + \sum_{l' \neq l} \exp\left(\left(-c_d d_{l,l'} + \beta V_{l',y}\right)/\sigma_\epsilon\right)} \tag{A-2}$$

$$P_{l,l,y} = \frac{\exp\left(\left(b_{stay} + \beta V_{l,y}\right)/\sigma_\epsilon\right)}{\exp\left(\left(b_{stay} + \beta V_{l,y}\right)/\sigma_\epsilon\right) + \sum_{l' \neq l} \exp\left(\left(-c_d d_{l,l'} + \beta V_{l',y}\right)/\sigma_\epsilon\right)} \tag{A-3}$$

6. Compute the likelihood:

$$L = \sum_y \sum_l \sum_{l'} \log P_{l,l',y}^{n_{l,l',y}} \tag{A-4}$$

Here, the value $n_{l,l',y}$ is the number of observations (i.e. months) that I observe a type-y rig move from location l to location l'.

C.2 Algorithm for computing the demand-side equilibrium

C.2.1 Overview

In the second step of the estimation I use the simulated method of moments to compute the parameters underlying the demand-side of the model. Here I set out the algorithm to compute the demand-side equilibrium that I recompute at every iteration of the objective function.

Note that rig costs are known from the first step of the estimation. I also know the empirical total number of rigs in each location $n_{l,y}$. Given these objects, and candidate match value parameters and the demand parameters, I compute an equilibrium as a fixed point in the probability a project matches with each capital type $\{q_{l,y}^{project}\}_{y \in \{low,mid,high\}}$.

Note that the demand-side equilibrium computation is separable over each location (since I fix the equilibrium number of rigs $n_{l,y}$ in each location). Therefore, the following algorithm centers on how to compute the equilibrium in one location. I set out the algorithm here, and then provide more details on the matching simulation below.

C.2.2 Demand-side algorithm

1. Guess the matching probability $\{q_{l,y}^{project,k}\}_{y \in \{low,mid,high\}}$ where k denotes the iteration and $k = 0$ denotes the initial guess.

2. Since rig costs are known, and for a candidate vector of demand-side parameters and the $q_{l,y}^{project,k}$, I can compute prices using the Nash Bargaining solution. Therefore, I can compute the value of a project of type x targeting a rig of type y using Equation (1): $\Pi_{l,x,y}^{project}$.

3. Update the probability of a project matching in the type-y rig submarket to iteration $k+1$, $\{q_{l,y}^{project,k+1}\}_{y \in \{low,mid,high\}}$, using a *matching simulation* (detailed below).

4. Iterate from Step 2 until convergence.

C.2.3 Matching simulation

The matching process outlined in the paper fits into a queuing framework for each rig y submarket. As mentioned in the main text, this queue is defined in Kendall's notation by $M/\tau/n_{l,y}/(n_{l,y}t_{backlog}/\tau)/FIFO$. That is, the queue has a Poisson arrival rate, service time at the contract duration τ, $n_{l,y}$ 'servers', $n_{l,y}t_{backlog}/\tau$ places in the queue, and a queuing discipline of first-in-first-out.

Denote the iteration of the queue by h, where an 'iteration' can be though of as a snapshot of the queue in a particular time period (a month) and an update to $h+1$ of the queue can be though of as the transition of the queue to the next time period. I simulate the queue for each rig type y submarket, in each location l, in the following way:

1. Initialize the backlog of each of the $n_{l,y}$ rigs at 0. Therefore the state of the queue is a $n_{l,y}$-length vector where each element is the backlog of a particular rig. Denote each element (for the i-th rig) by $b_{l,y}^{i,h}$.

2. Denote the realization of the number of wells in iteration h who enter by d_l^h. Compute this d_l^h by taking a draw from $Poisson(\lambda_l)$.

3. Take d_l^h draws from the project complexity distribution $f_{l,x}^{entry}$. Denote the type of each of these draws by $x_l^{j,h}$.

4. For each complexity draw $x_l^{j,h}$, compute the payoff to matching with each particular type of rig using Equation (1). (Note here that the ϵ_y draws in Equation (1) are project j and rig type y specific.)

5. For each j, find the rig type y where the payoff to matching is maximized. Denote the total number of wells that target rig type y by $d_{l,y}^h$. Then, compute matches:

   - If the number of wells $d_{l,y}^h$ is less than or equal to the total number of available rigs, then all wells will match with a rig. Therefore, add the contract length τ to the backlogs of $d_{l,y}^h$ available rigs. Note that in this iteration of the queue the probability of a well matching will be equal to 1.

- If the number of wells $d_{l,y}^h$ is greater than the number of available rigs, then not all of the wells will match. In this case, allocate wells to available rigs in the order of entry until the backlogs are completely full (i.e. adding one more match with contract length τ would cause the backlog of a rig to be greater than the critical value $t_{backlog}$). Note that in this iteration of the queue the probability of a well matching will be less than 1.

6. Update the queue to the next period $h+1$ by removing 1 month of each rig i with a backlog > 1 (backlogs cannot be negative so if the current backlog is 0, there will be no change in $b_{l,y}^{i,h}$).

7. Repeat from Step 2.

In practice, I start by 'burning-in' the matching simulation to remove dependence on the initial guess. I then iterate over h in the above algorithm many times. From this, I generate the long-run probability of a project matching in the type-y capital submarket ($q_{l,y}^{project}$), which is then used in the demand side algorithm. As a side-product, the queuing algorithm also delivers $q_{l,y}^{capital}$, rig utilization (the proportion of rigs with a positive backlog), and the average match for each rig type, amongst other things. These objects are useful for computing counterfactuals and moments in the demand estimation.

C.3 Algorithm for computing the counterfactuals

C.3.1 Overview

Overall, the algorithm for the counterfactuals involves recomputing the entire equilibrium of the global market for deepwater rigs. Unlike in estimation, I can no longer leverage empirical objects in the data like empirical probabilities of matching, because these will change in the counterfactuals.

One implementation of a full solution algorithm would be to iterate over the full demand-side equilibrium and the full supply-side equilibrium until convergence. While this would work in theory, in the context of the model in this paper it would be very computationally

demanding. The reason comes from computing the demand-side equilibrium: due to the two-sided vertical heterogeneity, and the queuing model which needs to be computed via simulation, the demand-side equilibrium is computationally slow.

Instead, I employ a slightly different algorithm. This algorithm still converges to the same equilibrium as a full-solution algorithm. It also preserves the broad idea of sequentially iterating over the demand-side and the supply-side of the model. However, I add in an extra step where I perturb and approximate the demand-side equilibrium before computing the supply-side equilibrium. In the algorithm this allows me to update — for each outer loop iteration — the supply-side equilibrium (which is computationally fast) multiple times for each single update of the full demand-side equilibrium (which is computationally slow). To put it another way, in the algorithm, the supply-side therefore is nudged faster towards to full-solution equilibrium, requiring less overall computations of the demand-side equilibrium.

To build further intuition about how the algorithm fits together, note that the demand side is separable across locations for a fixed number of rigs of each type in a location l. Therefore, the equilibrium in each location l on the demand side can be computed in parallel in each outer loop step. Furthermore, the supply side is separable across rig types y given the rig's probability of matching in each location and the average price of each rig once matched. Therefore, the supply side can be computed in parallel across rig types.

C.3.2 Algorithm

1. Initialize the algorithm at iteration $k = 0$ with a guess of the number of rigs of type y in each location l, denoted $n_{l,y}^{k=0}$. Also guess the probability of a project matching in each rig type y submarket in each location $q_{l,y}^{project,k=0}$.

2. For each location l, compute the demand side equilibrium at $n_{l,y}^{k=0}$ and also for "perturbations" around $n_{l,y}^{k=0}$:

   - To compute the perturbations, I use the demand-side algorithm detailed above in Section C.2.

- These perturbations correspond to varying the number of rigs of a particular type, holding the number of other rigs fixed *and* the $q_{l,y}^{project,k}$ fixed when projects make their targeting choices. Since $q_{l,y}^{project,k}$ is fixed, this requires computing steps 2. to 5. in the demand-side algorithm only once, and therefore computing the matching simulation only once.

- For each perturbation, and for each rig type y, record the equilibrium price and the probability of a rig matching.

3. Given these perturbations, update the supply side for each rig type y *across* locations in the following way.[2] Note that the following is an inner loop which iterates over the distribution of rigs in each location, and I denote the iteration of this inner loop by h.

   (a) Initialize the inner loop at $h = 0$ using the current distribution of rigs across space $n_{l,y}^{h=0}$.

   (b) Using linear interpolation over the perturbations computed in Step 2., get the expected price in each location, as well as the probability of matching for rigs.

   (c) Using these prices and the probabilities of matching, get the rig value functions $U_{l,y}^h$, $V_{l,y}^h$ and the corresponding conditional choice probabilities using the supply side algorithm in Section C.1.

   (d) Using the conditional choice probabilities, construct a transition probability matrix (i.e. a matrix where each row is the probability that a type y rig in location l will move to an alternative location l').

   (e) Update the number of rigs in each location *once* to produce a new distribution of rigs across locations $n_{l,y}^{h+1}$.

   (f) Repeat from sub-step 3(b) until convergence of the distribution of rigs of type y across locations.

---

[2]So, I run the following steps for each $y \in \{low, mid, high\}$

4. Given the new supply-side equilibrium, update the demand side equilibrium using the demand-side algorithm detailed above in Section C.2.

5. Repeat from step 2. until convergence in the distribution of rigs across space in the outer loop.

D Identification: details

D.1 Supply side: Substep 1.1

Here I provide more formal details about how the markup parameters $\delta_{l,y}$ as well as the shocks σ_ϵ and the value of staying in a location b_{stay} are identified using the location choice data alone.

Suppose that there are $n \geq 3$ locations and focus on identifying the parameters for a particular rig type y. There are $n+2$ distinct parameters to identify: one markup parameter for each of the n locations as well as b_{stay} and σ_ϵ. In each location there are n choice probabilities (the rig can choose to stay or move to one of the $n-1$ different locations), and $n-1$ degrees of freedom since these probabilities must sum to 1. This leads to $n(n-1)$ degrees of freedom in total. So long as the number of locations $n \geq 3$ then $n(n-1) \geq (n+2)$ and the parameters are identified.

E Equilibrium with two-sided heterogeneity

A key difference between the model in this paper and past work which studies markets where agents are relatively homogeneous (such as bulk shipping in Brancaccio et al. (2020)) is that I allow for two-sided vertical heterogeneity. Although this feature is important to understanding capital relocation in the offshore oil and gas industry, it adds substantial complexity to the equilibrium. In particular — with two-sided heterogeneity in the model — the entry of different types of rigs within a location will change relative prices and relative capacity constraints. As a result, potential projects may change their targeting behavior, thereby causing a reallocation of matches. This within-location equilibrium then affects capital location choices since it determines equilibrium prices and utilization. To highlight intuitively how two-sided heterogeneity shapes the within-

Figure A-2: Within-location equilibrium: effects of high-type capital entry

(a) P(target low-type | x) (b) P(target mid-type | x) (c) P(target high-type | x)
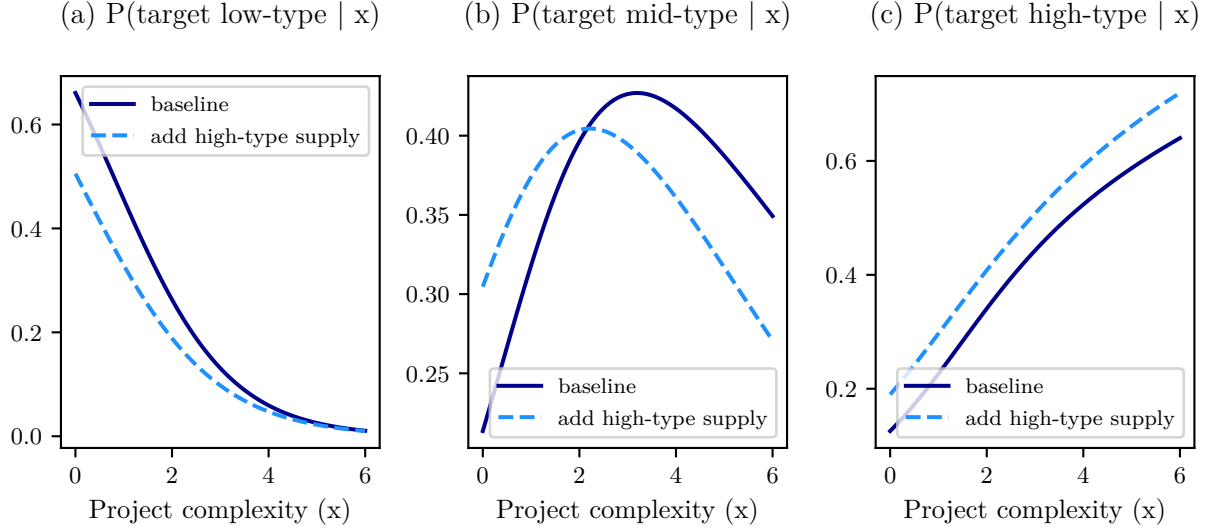
Note: This figure is a comparative statics exercise that shows the effect of a increase in high-type capital on the equilibrium targeting behavior of potential projects within a location. Recall that each potential project chooses — given prices and the probability of matching each type of capital $q_{l,y}^{project}$ — which type of capital to target using a logit model. This figure illustrates this targeting behavior: conditional on an project complexity type (x) on the x-axis, the y-axis shows the probability that it targets a particular type of capital. (So, for each x, these graphs can be summed vertically so that $1 = P(\text{target low-type }|x) + P(\text{target mid-type }|x) + P(\text{target high-type }|x)$.) The main point this figure highlights (discussed further in the text) is that high-type capital entry affects the targeting behavior of potential projects by changing equilibrium prices and relaxing capacity constraints. In equilibrium this reallocates matches from existing mid and low-type capital to high-type capital, and also affects sorting behavior within the location.

location equilibrium I perform a comparative statics exercise in Figure A-2.

Figure A-2 shows the probability that each type of potential project (on the x-axis) targets a particular type of capital within a location. In the baseline (shown by the solid dark-blue line) simple projects tend to target low-type capital, average complexity projects target mid-type capital, and complex projects target high-type capital. Next I consider the effects after an increase in high-type capital, shown by the dashed light-blue line. Initially, the entry of high-type capital relaxes the high-type capacity constraints and lowers high-type prices. This causes projects to redirect their targeting towards high-type capital and away from mid-type and low-type capital, resulting in an upwards shift of the dashed light-blue line. This then relaxes the mid-type capacity constraint and lowers the

mid-type price, which causes a further equilibrium shift in project targeting behavior away from low-type capital and towards mid-type capital. Notably, simple projects are *more likely* to target mid-type capital after high-type entry. Overall, the entry of high-type capital reduces prices and relaxes capacity constraints for all capital types, and causes all types of capital to be reallocated towards relatively simpler types of projects.

F Additional tables and figures

Table A-1: Fit of the moments: simulated vs data

	Simulated	Data		Simulated	Data
US			**Australia**		
Av. Price: Low	0.23	0.23	Av. Price: Low	0.27	0.27
Av. Price: High	0.40	0.40	Av. Price: High	0.47	0.46
Utilization	0.83	0.85	Utilization	0.91	0.93
Av. complexity: Low	1.20	1.18	**Central Americas**		
Av. complexity: Mid	2.75	2.74	Av. Price: Low	0.23	0.23
Av. complexity: High	3.69	3.70	Av. Price: High	0.52	0.53
$\beta_{0,low}$	0.29	0.27	Utilization	0.90	0.90
β_1	-0.06	-0.04	**Europe**		
β_2	0.07	0.05	Av. Price: Low	0.31	0.31
Africa			Av. Price: High	0.48	0.48
Av. Price: Low	0.30	0.29	Utilization	0.91	0.91
Av. Price: High	0.46	0.47	**Mediterranean**		
Utilization	0.85	0.86	Av. Price: Low	0.23	0.22
Asia			Av. Price: High	0.44	0.42
Av. Price: Low	0.23	0.22	Utilization	0.88	0.89
Av. Price: High	0.47	0.45	**South America**		
Utilization	0.83	0.83	Av. Price: Low	0.22	0.19
			Av. Price: High	0.43	0.43
			Utilization	0.93	0.93

Note: This table shows the fit of the simulated moments vs the empirical moments in the data. The simulated method of moments procedure is performed independently for each location starting with the US market.
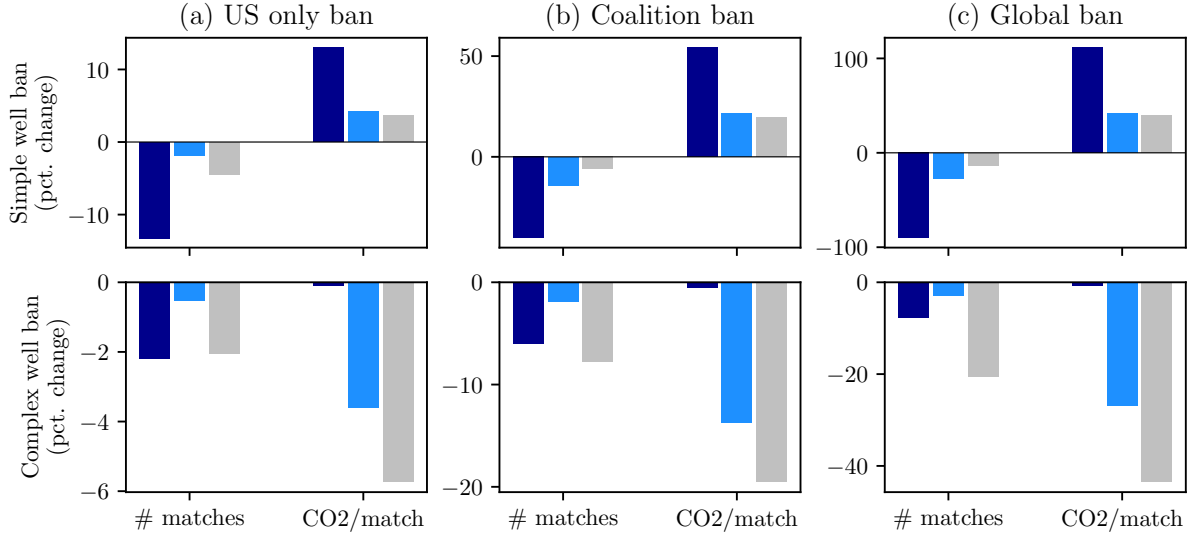
Figure A-3: Fit to untargeted moments
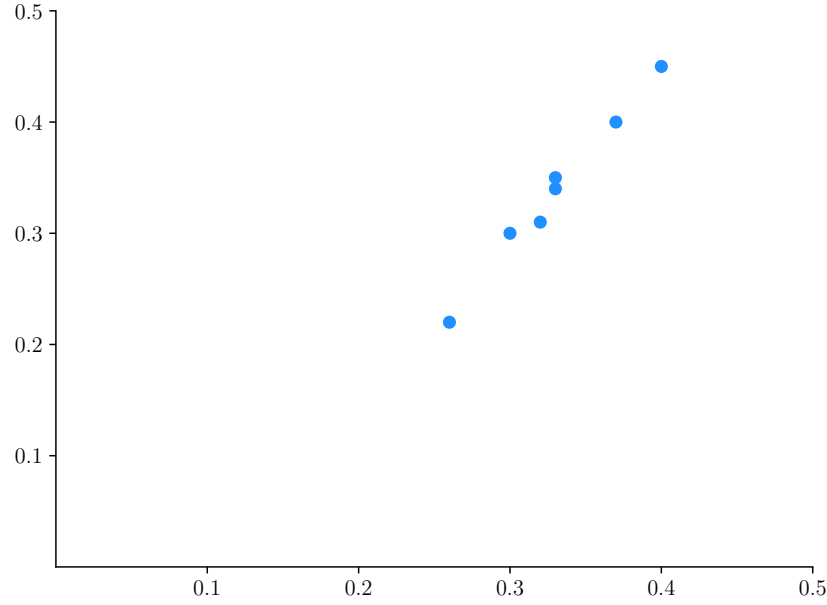
Note: This table shows the fit of the simulated untargeted moments vs the empirical untargeted moments in the data. Each dot represents the average price for a mid-specification rig in a location (with the exception of the US which is a targeted moment).

Figure A-4: Heterogeneous effects of regulation: detail

Note: Gray bar: change for high-specification rig. Light-blue bar: change for mid-specification rig. Dark-blue bar: change for low-specification rigs. Overall, this figure shows detail about the change in the carbon emissions per match, and also the number of matches, for all the six counterfactuals. The top row corresponds to the simple well ban counterfactuals and the bottom row corresponds to the complex well ban counterfactuals.

Table A-2: Estimation results: costs detail

| | Drilling cost $(c_{l,y} = \gamma \bar{p}_{l,y})$ | | |
| | Low-type | Mid-type | High-type |
	$c_{l,low}$	$c_{l,mid}$	$c_{l,high}$
Africa	0.155	0.188	0.250
	(0.1528, 0.1577)	(0.1844, 0.1903)	(0.2461, 0.2540)
Asia	0.118	0.160	0.242
	(0.1157, 0.1194)	(0.1578, 0.1628)	(0.2378, 0.2454)
Australia	0.147	0.166	0.245
	(0.1443, 0.1489)	(0.1630, 0.1682)	(0.2404, 0.2481)
Central Am.	0.120	0.240	0.283
	(0.1184, 0.1222)	(0.2360, 0.2435)	(0.2784, 0.2873)
Europe	0.168	0.211	0.255
	(0.1647, 0.1699)	(0.2078, 0.2145)	(0.2506, 0.2587)
Mid. East	0.116	0.183	0.224
	(0.1138, 0.1175)	(0.1798, 0.1855)	(0.2201, 0.2271)
South Am.	0.102	0.118	0.227
	(0.1003, 0.1035)	(0.1158, 0.1195)	(0.2236, 0.2307)
US	0.121	0.164	0.215
	(0.1190, 0.1228)	(0.1616, 0.1667)	(0.2110, 0.2177)

Note: Confidence intervals at 95% using 200 bootstrap replications in brackets.

References

Ahlvik, Lassi, Jørgen Juel Andersen, Jonas Hamang Hvending, and Torfinn Harding, "Quantifying Supply-side Climate Policies," *Working Paper*, 2022.

Brancaccio, Giulia, Myrto Kalouptsidi, and Theodore Papageorgiou, "Geography, Transportation, and Endogenous Trade Costs," *Econometrica*, March 2020, *88*, 657–691.

Kaiser, Mark, "A Survey of Drilling Cost and Complexity Estimation Models," *International Journal of Petroleum Science and Technology*, 2007, *1* (1), 1–22.

Vreugdenhil, Nicholas, "Booms, Busts, and Mismatch in Capital Markets: Evidence from the Offshore Oil and Gas Industry," *Working Paper*, 2023.